Available online at www.sciencedirect.com

SCIENCE DIRECT®

Journal of Molecular Catalysis A: Chemical 204–205 (2003) 581–589

JOURNAL OF MOLECULAR CATALYSIS A: CHEMICAL

www.elsevier.com/locate/molcata

Reaction and deactivation study of mesoporous silica–alumina (MSA) in propene oligomerisation

C. Flego*, S. Peratello, C. Perego, L.M.F. Sabatino, G. Bellussi, U. Romano

EniTecnologie SpA, via Maritano 26, I-20097 S. Donato Mil. (MI), Italy

Received 19 September 2002; received in revised form 7 February 2003; accepted 20 February 2003

Dedicated to Professor Renato Ugo on the occasion of his 65th birthday

Abstract

The deactivation of mesoporous silica–alumina (MSA) catalyst was investigated in the propene oligomerisation. Three catalysts with different acid site distribution were synthesised and tested, in order to determine the role of the acid sites in both main and side reactions. The initial activity is correlated with the Lewis acid site density. A two-stage mechanism for deactivation has been proposed. At the beginning of the reaction, poisoning of the active site takes place, the decay rate being consistent with the strength of the Lewis acid sites. At longer reaction time pore blockage, caused by an increasing of the dimensions of the adsorbed organic residues, becomes the main side phenomenon.

Keywords: Propene oligomerisation; Deactivation; Mesoporous silica–alumina (MSA); Acidity

1. Introduction

Organic reactions catalysed by solid acids are usually accompanied by the formation of by-products, bulkier than the reactants and the products, which cause the catalyst deactivation, by both poisoning of the active sites and/or blockage of the catalyst pores [1]. The deactivation can be, therefore, considered the result of a large number of side reactions (e.g. oligomerisation, dehydrogenation, cyclisation, alkylation), leading to the formation of polyaromatics and polyalkylaromatics, heavy by-products usually named "coke precursors" [2]. These reactions are deeply affected by the availability of catalytic sites, the spatial constraints of the catalyst [3–7], and the reaction parameters [8,9].

As a consequence of the formation of coke deposits, the catalytic performance decreases or collapses and the catalyst must undergo to regeneration. Unfortunately, the regeneration procedures (mainly thermal treatments in oxidising atmosphere) may cause detrimental effects on both the structure and the texture of the catalyst [10].

The oligomerisation of light olefins by solid acid catalysts is of industrial interest for the production of petrochemicals and fuels. Beside zeolites and supported phosphoric acid, a new amorphous mesoporous silica–alumina (MSA) has been recently developed and tested in propene oligomerisation, showing outstanding catalytic activity towards highly branched oligomers [11]. MSA [12] is an amorphous silica–alumina prepared by sol–gel in presence of tetrapropylammonium hydroxide (TPAOH) as tem-

* Corresponding author. Tel.: +39-02-52046678; fax: +39-02-52056364.
E-mail address: cflego@enitecnologie.eni.it (C. Flego).

1381-1169/$ – see front matter © 2003 Elsevier Science B.V. All rights reserved.
doi:10.1016/S1381-1169(03)00341-8

plate. The pore size distribution is very narrow and centred at ca. 40 Å mean pore width. Most of the Al atoms are in tetrahedral coordination, therefore, MSA displays good properties as acid catalyst.

The aim of this paper is to study the influence of the sole acidity (type, number and strength) on propene oligomerisation and simultaneously on the initial and steady state formation of carbonaceous deposits. As coke formation has been found to be a shape selective reaction, three MSA samples with constant pore structure and different acidity distribution were chosen.

2. Experimental

Catalysts and reactants: The preparation of mesoporous silica–alumina (MSA) samples was performed as described in [12,13], using $Si(C_2H_5O)_4$ (Dynasil-A, Nobel), $Al(iC_3H_7O)_3$ (Fluka), 15 wt.% aqueous solution of TPAOH containing <20 ppm of alkali cations. The synthesis of SiO_2/Al_2O_3 molar ratio was 50 for all samples. The silica source was added to the aqueous solution of TPAOH and aluminium alkoxide. Upon hydrolysis and condensation of the alkoxides, the two liquid immiscible phases were transformed into a clear viscous sol, and then into a homogeneous lightly opalescent gel by partial evaporation of the solvent. After 15 h ageing at room temperature, the gels were dried at 90 °C in N_2 flow for 24 h and calcined 6 h in air at 550 °C. By a proper combination of temperature and stirring during hydrolysis and condensation, silica–alumina materials (labelled MSA1, MSA2, MSA3) were obtained with comparable BET surface area (778, 764 and 806 m^2/g, respectively).

An extrudate catalyst, named MSAE, was obtained from MSA1 by extrusion (39 wt.%) with pseudobohemite (Versal 150), following the procedure described in [14].

High purity (99.5%) propene (SIAD) was used without further purification. Pyridine (Fluka) was distilled, dehydrated and purified by cryopumping before use.

Catalytic test: Runs were performed in a continuous flow fixed-bed reactor at the following conditions: temperature, $T = 155$ °C; total pressure, $P = 35$ bar; feed $C_3H_6/C_3H_8 = 70/30$ (wt/wt); weight hourly space velocity, WHSV = 4 h^{-1}.

UV-Vis and FT-IR experiments: For the FT-IR (Perkin-Elmer Model 2000) spectroscopic studies self-supported wafers were pressed from the powders with a thickness of 10–15 mg/cm^2. The wafers were placed into a sample holder inside a pyrex glass cell with KBr windows. This set-up allows the pre-treatment of the sample (300 °C, 2 h, N_2 and 300 °C, 1 h, vacuum $<10^{-3}$ mbar), the introduction of the probes and the heat treatments. The spectra were registered at 21 °C. Two different IR experiments were performed:

(i) acidity determination by pyridine adsorption at 200°C for 1 h and desorption at 200 and 300 °C for 1 h in vacuum. The acid sites density was determined from the intensity of the IR signals at 1455 cm^{-1} (pyridine coordinatively bonded to Lewis sites) and 1545 cm^{-1} (pyridinium ion), taken the extinction coefficients of [15];
(ii) propene adsorption at 150 °C followed by detection of surface species formed with time. After each set of IR measurement the same sample was analyzed by UV-Vis spectroscopy.

UV-Vis spectra (Perkin-Elmer Lambda 19 equipped with a 60 mm reflectance sphere) were registered in reflectance (Kubelka–Munk function, resolution 1 nm) using a evacuable Suprasil quartz cell. Powdered samples (ca. 500 mg) were placed into the cell and pretreated as for IR experiments. The measurements were performed, monitoring the generation of surface species with increasing: (i) time and (ii) temperature.

TG–DSC experiments: Twenty milligrams of powder were put in a quartz holder of a thermogravimetric–calorimetric system (TG–DSC 111 Setaram). The experiments were performed from 25 to 800 °C in air and N_2 (0.40–1.50 ml/s) at different scanning rate (2, 5, 10 and 20 °C/min) in order to determine the energetic parameters.

TPD experiments: TPD spectra in He flow (0.12 ml/s) from 25 to 900 °C (scanning rate, 10 °C/min) were registered by a mass spectrometer (QTMD 150 Carlo Erba). Before desorption, the pretreated samples (300 °C, 1 h, vacuum $<10^{-5}$ mbar) were contacted with 30 Torr of propene for 1 h at different temperatures (120, 150 and 200 °C) followed by evacuation at 25 °C for 10 min in vacuum and for 1 h in He flow.

Table 1
Acid site distribution and kinetic parameters of propene reaction

Sample	Brønsted acid (μmol/g)	Lewis acid (μmol/g)	a (g_{MSA} bar/mol)	$1/b$ (mol/(g_{MSA} bar h))
MSA1	167	72	2.28	5.2 E-03
MSA2	74	111	1.23	5.8 E-03
MSA3	52	164	0.45	11.0 E-03
MSA3*	54	118		
MSAE	21	253		
MSAE/d	0	171		
MSAE/d[a]	9	198		
MSAE/d[b]	22	211		

a, decay rate; $1/b$, initial activity.
[a] After thermal treatment in N_2.
[b] After thermal treatment in air.
* After contacting propene at 150 °C for 6 h.

3. Results and discussion

3.1. Acidity determination

The total acid site density of the three catalysts is reported in Table 1. The density of Lewis acid sites increases, and that of Brønsted acid sites decreases, in the order: MSA1 < MSA2 < MSA3. MSA3, after treatment with propene for 6 h at 150 °C, contains only small amount (<10%) of light organic compounds (from UV-Vis-IR analysis) and moisture and any aromatic species. The acidity determined in this material shows a lower density of Lewis acid sites and a similar one of Brønsted type with respect to the untreated sample. Acidity measurements were also performed on the extrudate catalyst, both fresh (MSAE) and as obtained after 10 days of continuous operation in the oligomerisation of propene at the conditions reported in Section 2 (MSAE/d). The different acid site distribution between MSA1 and MSAE is due to the dilution of the active phase with alumina precursor during extrusion, with decreasing of the Brønsted acid and increase of the Lewis acid sites. This discharged sample was also divided in different portions, treated up to 550 °C in N_2 (MSAE/d[a]) and in air flow (MSAE/d[b]), respectively. In MSAE/d are present only few Lewis acid sites, whose amount increase after both thermal treatments (MSAE/d[a] and MSAE/d[b]). No Brønsted acidity is detected in the discharged catalyst MSAE/d, restored partially and completely after thermal treatment in N_2 and in air, respectively. This is in agreement with the absence of IR bands in the structural hydroxyls region of the discharged samples and their reappearance after thermal treatments, partially after N_2 and completely after air treatments.

3.2. Adsorption of propene

Adsorption of propene was performed at 150 °C on MSA samples activated at 300 °C in N_2.

The IR spectra in the hydroxyl vibration region showed two signals with maximum at 3740 (external isolated silanols) and at 3650 cm^{-1} (OH groups involved in H bond). Adsorption of 1 Torr propene at 150 °C gave rise to new bands in: (i) 3000–2700 cm^{-1} range, characteristic for symmetric and asymmetric stretching vibrations of CH_2 (2850 and 2930 cm^{-1}) and CH_3 groups (2890 and 2960 cm^{-1}, respectively); (ii) 1650–1600 cm^{-1}, due to the C=C stretching and (iii) 1500–1300 cm^{-1} range, corresponding to symmetric and asymmetric bending vibrations of the CH_2 and CH_3 groups.

Immediately after loading of propene on MSA samples, bands due to $–CH_2–$ and $–CH_3$ group vibrations appear and increase with contact time. In the first 20 min the adsorption rate of organic species is high, then slows down. The evolution of the intensity of the IR bands due to $–CH_3$ and $–CH_2–$ is shown in Fig. 1A: the amount of $–CH_3$ groups increases faster than that of $–CH_2–$ groups. At a given time, the amount of paraffinic compounds (from 3000–2800 cm^{-1} region) increased in the following order: MSA1 > MSA2 > MSA3, similarly to the intensity of the $–CH_3$ group.

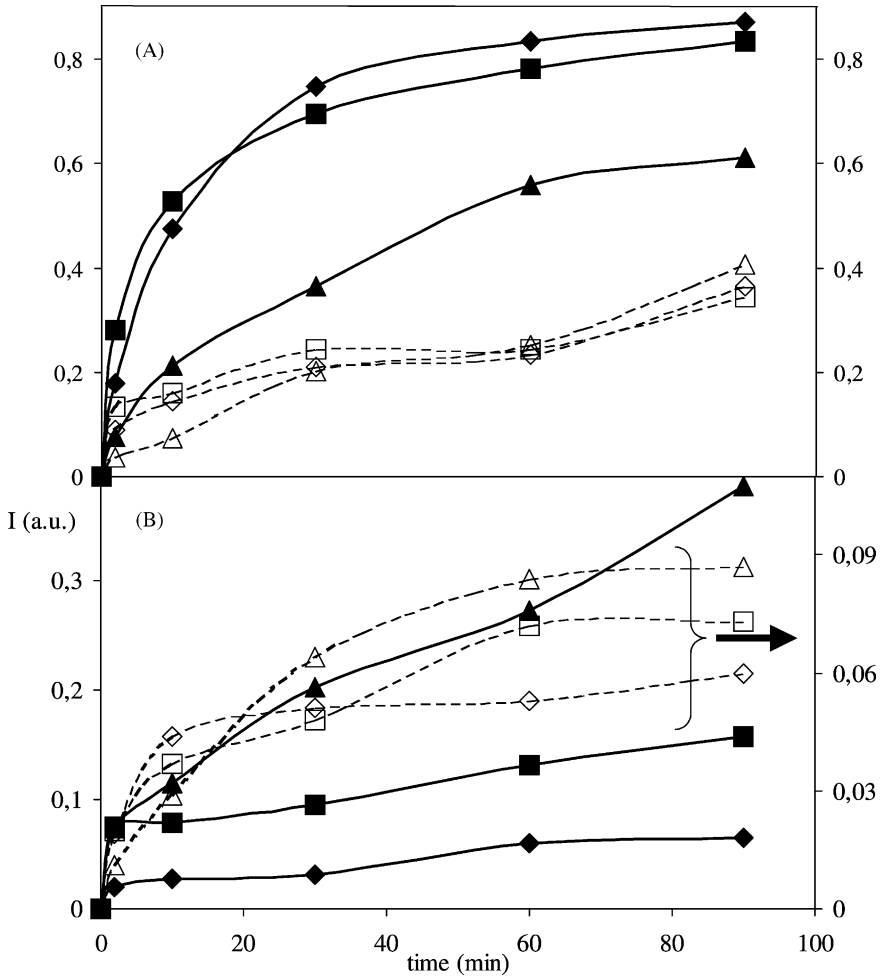

Fig. 1. Intensity evolution (a.u.) of the IR bands: (A) of methyl (plain line) and methylene (dotted line) groups; (B) in the 1675–1640 cm^{-1} (plain line) and 1400–1350 cm^{-1} (dotted line) range, after contacting MSA1 (◆), MSA2 (■) and MSA3 (▲) with propene at 150 °C.

In all MSA materials the IR signal in the 1650–1600 cm^{-1} range decreases in intensity with time. The maximum of this signal shifts with the catalyst, moving to 1607 ($\Delta\nu = -43\,cm^{-1}$), 1614 ($\Delta\nu = -36\,cm^{-1}$) and 1636 cm^{-1} ($\Delta\nu = -14\,cm^{-1}$) in presence of MSA1, MSA2 and MSA3, respectively. The shift to lower frequency with respect to the stretching position of the gas phase (1647 cm^{-1}) is due to the partial loss of the double bond character of the C=C bond after chemisorption on the active sites of the catalyst [16,17]. The extent of the shift is related to the Lewis acid strength of the active site [18]. From these evidences, the following ranking of the Lewis acid strength is determined by using propene as a probe: MSA1 > MSA2 > MSA3.

The intensity of the bands at lower frequency (1500–1300 cm^{-1}) grew with time (Fig. 1B for the integration range of 1400–1350 cm^{-1}). Same behaviour was found for the 1468–1470 cm^{-1} band, related to the deformation of CH group in oligomers [16,19]. The intensities ratio of the IR signals attributed to the presence of isopropyl and isobutyl groups (I_{1370}/I_{1386}) is a measure of the branching degree of organic compounds [20,21]. The intensity ratio for these IR signals are depicted and increase with time, in the order: MSA3 > MSA2 > MSA1.

At longer reaction time, IR bands characteristic of a CH= stretching (3100–3000 cm^{-1} range) and a new doublet (at 1649 and 1670 cm^{-1}) due to conjugated dienes develop [20,22]. The intensity of these IR bands (integration range of 1675–1640 cm^{-1} in Fig. 1B) was as follows: MSA3 > MSA2 > MSA1.

The UV-Vis spectra registered at the end of the "in situ" experiments with propene give information about the unsaturation degree of the organic residues: strong signals at 300, 373, 450 and 562 nm are due to mono-, di-, tri- and tetra-enyl carbenium ions [23,24], respectively. While in MSA1 the mono- (i.e. propene) and di-enylic species are prevalent, the intensity of the signals at lower energy (higher unsaturation degree) is higher in MSA2 and MSA3.

The evolution of the UV-Vis spectra after interaction of propene with MSA1 is reported in Fig. 2. After 5 min at 21 °C (20 Torr of propene), a shoulder is observed at 300, the intensity increasing with time. After contacting at 150 °C for 5 min a new band at around 370 nm and an additional shoulder at 480 nm develop together with that at 300 nm. At longer reaction time the intensity of all absorptions increased and further new bands are detected at lower energies, caused by the increase of unsaturation degree of the organic residues.

UV-Vis-IR spectroscopic analysis gives an overview on the nature of the organic species present on the catalyst during reaction. MSA2 and MSA3 present high amount of branched oligomers with a higher degree of unsaturation and a low formation of paraffinic species and unsaturated cycles. By contrast in MSA1 the presence of both branched species and enylic species is less relevant, while a large production of paraffinic compounds is observed.

3.3. Adsorption–desorption of propene

The release of the products of propene reaction was studied by TPD analysis after adsorption at different temperatures (120, 150 and 200 °C). By increasing the adsorption temperature, the amount of propene desorbed decreases (Table 2). At the same time the shape of propene profile and the intensity of the maximum gradually change. As a general feature, the desorption starts at ca. 120 °C with one maximum in the 270–285 °C range. Besides propene, methane (C_1) and $C_2 \cdots C_6$ alkenes are the main products detected by

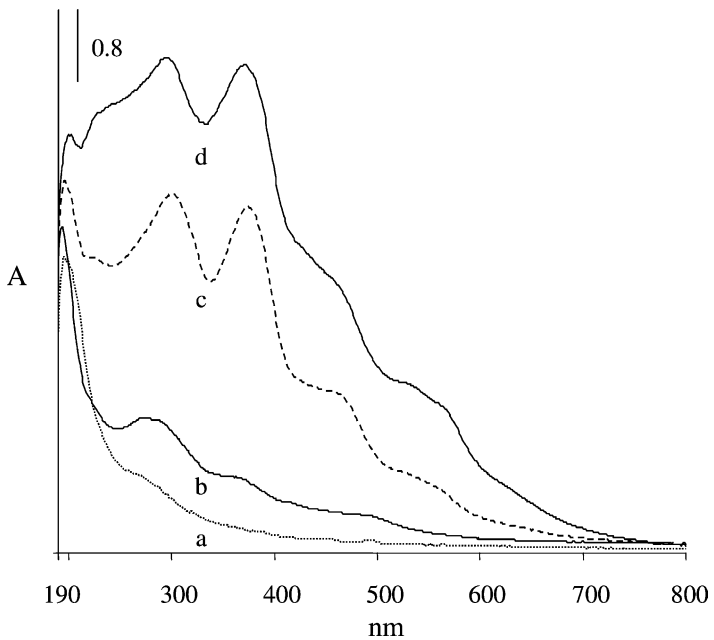

Fig. 2. UV-Vis spectra of MSA1 after contacting with propene at 25 °C for (a) 5 min and (b) 60 min and at 150 °C for (c) 5 min and (d) 30 min.

Table 2
Maximum of desorption (T °C) and normalised peak area (n.a.) of MSA samples after propene adsorption at 150 °C

Organic species	MSA1		MSA2		MSA3	
	T (°C)	n.a.	T (°C)	n.a.	T (°C)	n.a.
C_1	278	0.0296	278	0.0239	278	0.0256
C_2	286	0.0075	279	0.0882	273	0.0679
C_3	277	0.2382	276	0.1716	273	0.1560
C_3 (120)		0.2940		0.2259		0.3122
C_3 (200)		0.0841		0.0730		0.1010
C_4	276	0.0306	276	0.0253	273	0.0259
C_5	276	0.0114	276	0.0094	270	0.0100
C_6	274	0.0026	276	0.0020	270	0.0020
C_p	276	0.0005	279	0.0003	273	0.0003
C_b	296	0.0008	293	0.0009	296	0.0003

C_3 (120), after propene adsorption at 120 °C; C_3 (200), after propene adsorption at 200°C. C_p, methylcyclopentene; C_b, benzene.

TPD. After adsorption at 150 °C also methylcyclopentene and benzene are present. These simple cyclic compounds are considered precursors of polycyclic coke precursors, responsible of deactivation.

In Table 2, the temperature corresponding to the maximum of desorption and the normalised area of the peaks are reported. The three samples showed almost the same behaviour, but with respect to C_2 release, unusually low in MSA1.

The profiles of methyl group obtained after propene adsorption on MSA3 at the different temperatures are depicted in Fig. 3 and show two maxima at 280 and 510 °C. The higher the adsorption temperature, the lower is the intensity of the peak at 280 °C and the higher is that at 510 °C. Same behaviour is also found in MSA1 and MSA2. The shape of the first peak is similar to that of propene and the other alkenes desorption in the same range. It can be related to the cracking of the oligomers present on the catalyst. The methyl fragment measured by MAS detector at ca. 510 °C is related to the thermal cracking of a saturated chain formed by inter-chain hydride transfer [25].

Two different classes of organic compounds are identified in these catalysts: (i) alkenes with 2–6C atoms, desorbed in large amount (67% of the total weight loss) at low temperature (200–350 °C); (ii) oligomers and cyclic compounds in small amount, that are decomposed at high temperature (370–540 °C). Cyclic compounds as methylcyclopentene and benzene are considered products of a large number of side reactions, leading to polyalkylaromatics and polyaromatics (coke precursors) [27]. The tendency to form these heavy molecules is present in all samples, the

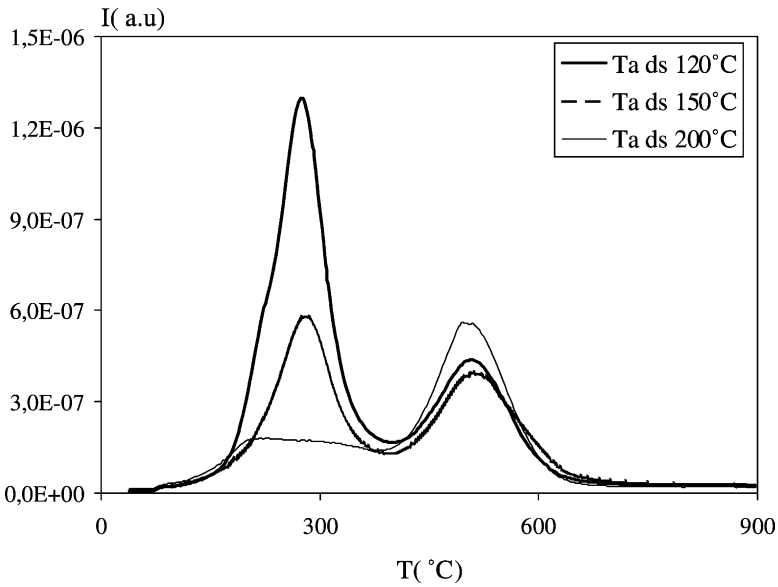

Fig. 3. TPD profiles of methyl group after adsorption of propene on MSA2 at (a) 120 °C, (b) 150 °C and (c) 200 °C.

Table 3
Thermogravimetric and calorimetric data of MSAE/d determined for different scanning rates

(°C/min)	T_{max1}	WL_1 (%)	T_{max2}	WL_2 (%)	Total WL (%)	E_{des}
Air						
2	52.8	13.64	482.1	6.14	28.79	E_1=36.191 kJ/mol; r=0.9959
5	72.3	12.58	490.3	8.57	26.71	
10	86.8	16.10	515.7	7.91	29.51	E_2=-159.504 kJ/mol; r=0.9576
20	110.3	15.71	484.1	3.66	21.43	
N_2						
2	57.6	12.81			22.89	E_1=37.158 kJ/mol; r=0.9606
5	88.8	12.21			20.37	
10	92.8	14.63			24.38	
20	114.4	10.03			17.76	

WL_1, weight loss at low temperature; WL_2, weight loss at high temperature; total WL, weight loss in the whole temperature treatment (25–800 °C).

ranking being the same as for the deactivation tendency: MSA1 > MSA2 > MSA3.

3.4. Desorption from spent catalysts

The weight loss due to organic species and the heat flow were measured in TG–DSC experiments of MSAE/d catalyst in air and N_2 (Table 3). The weight loss after thermal treatment in N_2 was 20–25% lower than that in air and carbonaceous residues were still present in the sample (as confirmed by the continuous absorption in the UV-Vis region). The energy (E_{des}) involved in these treatments was determined at different scanning rates, applying the Cvetanovic–Amenomiya equation [26]:

$$2\ln T_{max} - \ln\beta = E_{des}/RT_{max} + \ln(E_{des}/AR)$$

where β is the scanning rate; R the general gas constant; A the pre-exponential factor of the Arrhenius equation.

The first peak (T_{max} in the 50–110 °C range, E_{des} = 36.6 kJ/mol) was endothermic in both atmospheres, due to light organic compound and water release. The second peak (T_{max} in the 480–520 °C range, E_{des} = −160 kJ/mol) was exothermic, caused by coke combustion in air treatment.

3.5. Catalytic tests

The reactivity of MSA samples was followed under isothermal conditions, which allow the simultaneous determination of the kinetic parameters of both reaction and deactivation. The catalytic activity, studied in a plug flow reactor at the experimental conditions described in Section 2, was different for the three catalysts as shown by the conversion versus time on stream (t.o.s.) curves in Fig. 4. By using a first order reaction, the kinetic constant (k_{kin}) could be calculated according to the following equation:

$$\ln(1 - \eta_{C_3H_6}) = 42 p^{\circ}_{C_3H_6} k_{kin}/\mathrm{WHSV}$$

where $\eta_{C_3H_6}$ is the total propene conversion; 42 the propene molecular weight; $p^{\circ}_{C_3H_6}$ the propene partial pressure (bar) and WHSV the weight hourly space velocity (h^{-1}).

In order to describe the relationship between k_{kin} and t.o.s., thereby the deactivation, the following equation was used:

$$k_{kin} = 1/(a \times \text{t.o.s.} + b)$$

where a is the decay rate ($g_{catalyst}$ bar/mol); $1/b = k_{kin}$ (mol/(h $g_{catalyst}$ bar)) when t.o.s. = 0.

The model parameters were estimated by using a not linear least-square analysis. Fig. 4 reports the comparison between experimental points and calculated curves for the three catalysts. Deactivation parameters obtained for the three samples are reported in Table 1.

The comparison between kinetic parameters of catalytic deactivation test and acidity measurements (Table 1) evidences that: (i) the initial activity ($1/b$) is related to the density of Lewis acid sites, the higher the former, the larger is the latter; (ii) the deactivation

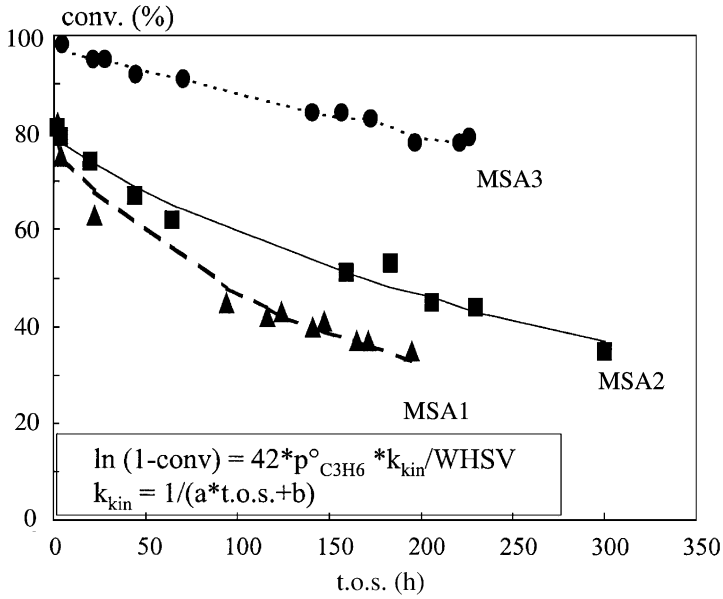

Fig. 4. Propene conversion, experimental (symbol) and calculated (curve) vs. time on stream for MSA1, MSA2 and MSA3 samples.

rate (*a*) increases with the density of Brønsted acid sites.

3.6. Mechanism of reaction/deactivation

All these experimental evidences allow drawing the following mechanism, in which both Lewis and Brønsted acid sites interact with propene, giving rise to different pathways.

The role of Lewis acid sites in oligomerization reaction is already reported in the literature [28,29]. In the early stage of reaction these are the active sites towards propene, responsible of the formation of branched oligomers, as confirmed by the fact that only Lewis acid sites are found bonded with organic species [30,31] at the beginning. The strength of this bond depends mainly on the acid strength of the sites and consequently the stronger Lewis acid sites are immediately "poisoned" by the reactant, causing a lower activity in the corresponding catalysts. This phenomenon is confirmed by both acidity measurements (Table 1) and catalytic performances (Fig. 4). The Brønsted acid sites, responsible of side reactions, are modified as well by the presence of propene derivatives, but their interaction is weak in the early stages (Table 1), as it is not possible to measure their different activity through the presence of different amount or type of side products.

The influence of the Brønsted acid sites on the reaction is, therefore, not observed in the earlier stage, while it becomes more evident at longer reaction times: propene reacts with Brønsted acid sites, giving alkenes, alkanes and aromatic compounds by hydride transfer [32,33]. In fact olefinic products formed on the Brønsted acid sites can either desorb as olefins by returning the protons to the catalyst or undergo the bimolecular hydrogen transfer. At low temperatures (i.e. 150 °C) it is reasonable to expect that olefin undergoes to saturation by hydrogen transfer [34]. The so formed paraffins are probably responsible of pore blockage, together with condensed aromatic compounds. This hinders any further interaction between reactant and Brønsted acid sites (presumably located in the inner part of the pores). At the external surface the Lewis acid sites continue to work.

According to the above evidences and to the TG–DSC experiments, a two-stage regeneration procedure can be suggested: (i) flowing N_2 to desorb the large amount of small organic compounds weakly bonded to the catalyst and (ii) combustion in air at ca. 500 °C of the heavy strongly bonded organic compounds.

4. Conclusions

In the propene oligomerisation catalysed by mesoporous silica–alumina (MSA), the formation of unsaturated carbenium ions is the first step which leads to catalyst deactivation. MSA with same porosity, but different acid sites distribution show different behaviour in the reaction: the higher the amount of Lewis acid sites, the higher is the initial catalytic activity and the formation of branched oligomers. The higher the amount of Brønsted acid sites, the faster is the deactivation rate and the formation of coke precursors.

Acknowledgements

The authors are indebted to Prof. I. Kiricsi for his interest in this work and for his helpful suggestions.

References

[1] A. Bellare, D.B. Dadyburjor, J. Catal. 140 (1993) 510.
[2] M. Guisnet, P. Magnoux, Appl. Catal. 54 (1989) 1.
[3] E.E. Wolf, F. Alfani, Catal. Rev. Sci. Eng. 24 (1982) 329.
[4] D.M. Bibby, N.B. Milestone, J.E. Petterson, L.P. Aldridge, J. Catal. 97 (1986) 493.
[5] S. Liu, S. Prasad, J. Wu, L. Ma, T. Yang, J. Chiou, J. Chang, T. Tsai, J. Catal. 142 (1993) 664.
[6] N. Mori, S. Nishiyama, S. Tsuruya, M. Masai, Appl. Catal. 74 (1991) 37.
[7] U.A. Sedran, R.A. Comelli, N.S. Figoli, Appl. Catal. 11 (1984) 227.
[8] P. Magnoux, P. Roger, C. Canaff, V. Fouche, N.S. Gnep, M. Guisnet, Catalyst Deactivation, in: B. Delmon, et al. (Eds.), Elsevier, Amsterdam, 1987, p. 317.
[9] V. Solinas, R. Monaci, E. Rombi, L. Forni, Catalyst Deactivation, in: B. Delmon, et al. (Eds.), Elsevier, Amsterdam, 1987, p. 493.
[10] K. Moljord, P. Magnoux, M. Guisnet, Catal. Lett. 25 (1994) 141.
[11] S. Peratello, M. Molinari, G. Bellussi, C. Perego, Catal. Today 52 (1999) 271.
[12] G. Bellussi, C. Perego, A. Carati, S. Peratello, E. Previde Massara, G. Perego, Zeolites and Related Microporous Materials: State of the Art, in: J. Weitkamp, et al. (Eds.), Elsevier, Amsterdam, 1994, p. 85.
[13] C. Perego, S. Peratello, R. Millini, EP 659478A1 (1993).
[14] G. Bellussi, C. Perego, S. Peratello, US 5342814 (1993).
[15] J. Take, T. Yamaguchi, K. Miyamoto, H. Okyama, M. Misono, Stud. Surf. Sci Catal. 28 (1986) 495.
[16] L. Kubelkova, J. Novakova, Z. Dolejsek, P. Jiru, Collect. Czechoslov. Chem. Comm. 45 (1980) 3101.
[17] H. Lechert, C. Dimitrov, C. Bezuhanova, V. Nenova, J. Catal. 80 (1983) 457.
[18] J. Datka, J. Chem. Soc., Faraday Trans. 1 77 (1981) 1309.
[19] V. Bolis, J.C. Vedrine, J. Chem. Soc., Faraday Trans. 1 76 (1980) 1606.
[20] S. Ceckiewicz, A. Baranski, J. Galuszka, J. Chem. Soc., Faraday Trans. 1 74 (1978) 2027.
[21] J. Datka, J. Chem. Soc., Faraday Trans. 1 76 (1980) 2437.
[22] J. Novakova, L. Kubelkova, Stud. Surf. Sci. Catal. 65 (1991) 405.
[23] I. Kiricsi, H. Forster, J. Chem. Soc., Faraday Trans. 1 84 (1988) 491.
[24] I. Kiricsi, H. Forster, Gy. Tasi, J. Mol. Catal. 65 (1991) L29.
[25] T.J. Gricus Kofke, R.J. Gorte, J. Catal. 115 (1989) 233.
[26] J. Cvetanovic, Y. Amenomiya, Appl. Catal. 17 (1967) 103.
[27] C. Flego, G. Pazzuconi, E. Bencini, C. Perego, Stud. Surf. Sci. Catal. 126 (1999) 461.
[28] K. Mizuno, M. Ikeda, T. Imokawa, J. Take, Y. Yoneda, Bull. Chem. Soc. (Jpn.) 49 (1976) 1788.
[29] J.P. Wolthnizen, J.P.van der Berg, J.H.C. van Hoff, Catalysis by Zeolites, in: B. Imelik, et. al. (Eds.), Elsevier, Amsterdam, 1980, p. 85.
[30] B.E. Langner, Ind. Eng. Chem. Process Des. Dev. 20 (1981) 326.
[31] B.E. Langner, J. Catal. 65 (1980) 416.
[32] J.F. Mc Mahon, C. Bednard, E. Solomon, Adv. Pet. Chem. 3 (1993) 285.
[33] A.K. Ghosh, R.A. Kydd, J. Catal. 100 (1986) 185.
[34] C.M. Tsang, P.-S.E. Dai, F.P. Mertens, R.H. Petty, in: Proceedings of the 208th Natational Meeting in American Chemical Society of Division of Petroleum Chemistry, Washington, August 1994, p. 367.